

Gas-Phase Catalytic Oxidation of CO by Au₂⁻

Hannu Häkkinen* and Uzi Landman

School of Physics
Georgia Institute of Technology
Atlanta, Georgia 30332-0430

Received June 28, 2001

Chemical reactivity of transition metal clusters toward various molecules in gas phase has been a subject of numerous investigations,^{1,2} motivated by search of analogues to adsorption mechanisms and reactivity at bulk metal surfaces. However, the full catalytic cycle, involving detection of a product molecule XY, as a result of reaction between reactants X and Y in the presence of the metal cluster M (possibly through an intermediate compound MXY), has been demonstrated experimentally only in a handful of studies.²

While it is well-known that gold is chemically inert as bulk material, nanometer-sized dispersed gold particles often show remarkable catalytic activity.³ Most recently it was found that mass-selected deposited gold clusters Au_N (N = 2 – 20) on MgO(001) exhibit extremely sensitive size-effects in the catalytic activity to oxidize CO: only clusters with eight or more atoms catalyzed the reaction, and the CO₂ yield had a nontrivial dependence on the cluster size for N ≥ 8.⁴ A concurrent theoretical study revealed that charging effects (by electrons trapped in surface color centers of MgO) are important in activating the gold cluster and the adsorbed O₂.⁴ It is then of interest to study also the reactivity and catalytic properties of small negatively charged gold clusters in the gas phase. Indeed, there are several experimental gas-phase studies⁵ on the reactivity of small anionic gold clusters with O₂ and CO.

We present here a detailed investigation, based on the density functional theory, on the interactions of oxygen and carbon monoxide with the gold dimer anion, which is the smallest gold cluster found to react with oxygen in the gas phase.⁵ We find that oxygen should bind molecularly to Au₂⁻. Furthermore, we studied a full catalytic cycle, producing two carbon dioxide molecules, and identified a key intermediate state, di-gold-carbonate, which should be detectable in the experiments.⁶

In this study the Kohn–Sham (KS) equations were solved using the Born–Oppenheimer local-spin-density molecular dynamics (BO-LSD-MD) method,⁷ including generalized gradient corrections (GGA),⁸ with nonlocal norm-conserving pseudopotentials⁹ for the 5d¹⁰6s¹, 2s²2p², and 2s²2p⁴ valence electrons of Au, C, and O atoms, respectively. Bonding in gold clusters requires a relativistic treatment;^{10,11} a scalar-relativistic¹² pseudopotential was

Table 1. GGA vs Experimental Data of Bonding

	S ^a	d (Å)	D (eV)	vIP (b) or vDE (c)(eV)
Au ₂	0	2.54 (2.47) ^b	2.22 (2.29) ^b	(b) 9.40 (9.16) ^c
Au ₂ ⁻	1/2	2.65 (2.58) ^b	1.81 (1.92) ^b	(c) 2.08 (2.01) ^{b,d}
AuO	1/2	1.91	2.36	(b) 9.94
AuO ⁻	0	1.91		(c) 2.31
CO	0	1.141 (1.128) ^e	11.06 (11.24) ^e	(b) 13.81 (14.01) ^f
O ₂	1	1.25 (1.21) ^e	5.36 (5.23) ^e	(b) 12.92 (12.06) ^f
CO ₂	0	1.18 (1.16) ^e	16.99 (16.87) ^{e,g}	(b) 13.63 (13.77) ^f

^a Shown are spin S, bond length d, dissociation energy D, and (b) vertical ionization potential, vIP, or (c) vertical electron detachment energy, vDE, for neutral and anionic systems, respectively. The experimental data is shown in parentheses. ^b Reference 14. ^c Reference 15 (adiabatic value). ^d Adiabatic EA from refs 14, 16 is 1.94 eV to be compared to 2.02 eV from theory. ^e Reference 17. ^f Reference 18. ^g Atomization energy.

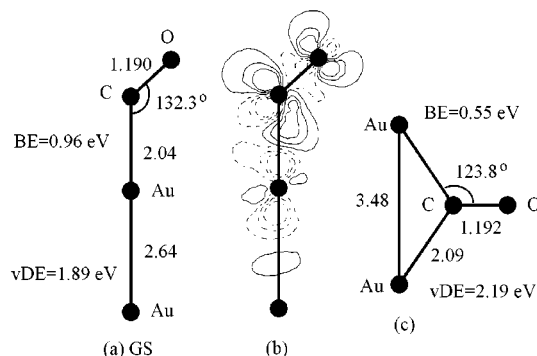


Figure 1. (a) Ground-state (GS) structure ($S = 1/2$) of Au₂CO⁻; (b) contour plot of density difference, $\Delta\rho = \rho(\text{Au}_2\text{CO}^-) - \rho(\text{Au}_2^-) - \rho(\text{CO})$; (c) “side-bonded” isomer ($S = 1/2$). BE is the binding (adsorption) energy of CO, vDE is the vertical electron detachment energy. The contours of $\Delta\rho$ are shown in the range of -0.015 – 0.015 au with 0.006 au intervals. Dashed (solid) line denotes depletion (accumulation) of the density. The indicated bond lengths are given in Å.

used here. From comparison of several calculated properties of basic dimers Au₂, Au₂⁻, AuO, AuO⁻, and molecules O₂, CO, as well as CO₂, to available experimental values in Table 1, we judge that calculations at the GGA level give a rather satisfactory description of the energetics and structure of these systems. The same methodology was used recently by us to study oxidation of CO at a single Pd atom adsorbed on a surface color center on a MgO(001) film,¹³ and the calculated reaction barriers agree favorably with the ones deduced from the experiment.¹³

We found two bonding configurations for Au₂CO⁻, shown in Figure 1. In the ground-state (GS) “end-bonded” configuration (Figure 1a) both the Au–Au and C–O bonds are significantly stretched. The calculated adsorption energy of CO is 0.96 eV. In the “side-bonded” configuration (Figure 1c), which is 0.41 eV less stable than the GS, the CO induces a break-up of the Au–Au bond. This illustrates the ability of CO to bind to different sites of the metal cluster, reminiscent of various adsorption sites on transition metal surfaces (e.g., on-top, bridge, etc.).

The bonding of CO to transition metal surfaces is generally characterized by charge transfer from the metal (donation) to the antibonding CO(π^*) orbital, and back-donation to the metal mainly from the bonding CO(σ) orbital.¹⁹ Similar concepts apply

(12) (a) Kleinman, L. *Phys. Rev. B* **1980**, *21*, 2630. (b) Bachelet, G. B.; Schluter, M. *Phys. Rev. B* **1982**, *25*, 2103.

(13) Abbet, S.; Heiz, U.; Häkkinen, H.; Landman, U. *Phys. Rev. Lett.* **2001**, *86*, 5950.

(14) Ho, J.; Ervin, K. M.; Lineberger, W. C. *J. Chem. Phys.* **1990**, *93*, 6987.

(15) Cheeseman, M. A.; Eyley, J. R. *J. Phys. Chem.* **1992**, *96*, 1082.

* Corresponding author. E-mail: hannu.hakkinen@physics.gatech.edu.

(1) Knickelbein, M. B. *Annu. Rev. Phys.* **1998**, *50*, 79.
 (2) Ervin, K. M. *Int. Rev. Phys. Chem.* **2001**, *20*, 127.
 (3) (a) Haruta, M. *Catal. Today* **1997**, *36*, 153. (b) Bond, G. C.; Thompson, D. T. *Catal. Rev.-Sci. Eng.* **1999**, *41*, 319.
 (4) Sanchez, A.; Abbet, S.; Heiz, U.; Schneider, W.-D.; Häkkinen, H.; Barnett, R. N.; Landman, U. *J. Phys. Chem. A* **1999**, *103*, 9573.
 (5) (a) Cox, D. M.; Brickman, R.; Creegan, K.; Kaldor, A. Z. *Phys. D* **1991**, *19*, 353. (b) Lee, T. H.; Ervin, K. M. *J. Phys. Chem.* **1994**, *98*, 10023. (c) Salisbury, B. E.; Wallace, W. T.; Whetten, R. L. *Chem. Phys.* **2000**, *262*, 131; (d) Bernhardt, Th.; Heiz, U. Private communication.
 (6) While at saturation two or more O₂ and CO molecules may adsorb on Au₂⁻, we limit ourselves here to the low-coverage regime.
 (7) Barnett, R. N.; Landman, U. *Phys. Rev. B* **1993**, *48*, 2081. This method does not use periodic boundary conditions for the ionic system.
 (8) Perdew, J. P.; Burke, K.; Ernzerhof, M. *Phys. Rev. Lett.* **1996**, *77*, 3865.
 (9) Troullier, N.; Martins, J. L. *Phys. Rev. B* **1991**, *43*, 1993. The core radii (in a₀) are: Au: s(2.50), p(3.00), d(2.00); C: s(1.50), p(1.54); O: s(1.45), p(1.45), with Au(s), C(p), and O(p) as local components. KS orbitals are expanded in a plane-wave basis with 62 Ry energy cutoff.
 (10) Häkkinen, H.; Landman, U. *Phys. Rev. B* **2000**, *62*, R2287.
 (11) Grönbeck, H.; Andreoni, W. *Chem. Phys.* **2000**, *262*, 1.

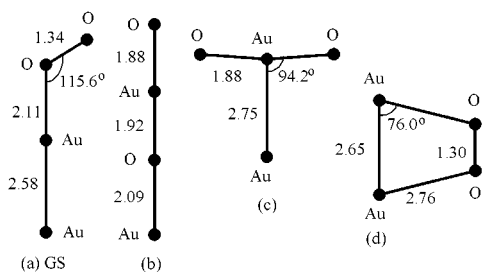


Figure 2. Four lowest-energy structures of Au_2O_2^- . The tilted “end-bonded” structure in (a) is the ground state. The binding (adsorption) energy per oxygen molecule, BE, the vertical electron detachment energy, vDE, and the spin S are: BE = 1.39 eV, vDE = 3.25 eV, $S = 1/2$ in (a), BE = 0.79 eV, vDE = 3.31 eV, $S = 3/2$ in (b), BE = 0.54 eV, vDE = 3.21 eV, $S = 1/2$ in (c), BE = 0.39 eV, vDE = 2.61 eV, $S = 1/2$ in (d). Bond lengths are given in Å.

here to the bonding of CO to Au_2^- , as can be seen in Figure 1b. Spatial analysis of the electronic charge reveals that 0.4e is donated to the $\text{CO}(\pi^*)$ orbital, accompanied by 0.24e back-donation to gold giving a net transfer of 0.16e to CO. This is reflected in the long bond length of CO and calculated vibration frequency²⁰ of 1841 cm^{-1} . A similar bonding mechanism applies for the “side-bonded” isomer (Figure 1c) but with a lesser amount of charge transfer. The calculated CO frequency is 1797 cm^{-1} . These results are to be compared to the GS neutral linear ($S = 0$) Au_2CO complex, for which the Au–Au, Au–C, and C–O bond lengths are 2.52, 1.93, and 1.149 Å, respectively, the CO adsorption energy is 1.60 eV, and vibration frequency is 2147 cm^{-1} . Summarizing, the extra electron of the anionic GS complex weakens both the Au–CO and C–O bonds, induces a large red-shift in the CO frequency, and causes a change in the structure, leading to the tilted adsorption geometry due to symmetry breaking by electron promotion to only one of the initially degenerate $\text{CO}(\pi^*)$ orbitals. Interestingly, while CO is traditionally considered to adsorb perpendicularly to a metal surface, in a recent STM study²¹ tilted adsorption geometries for CO ligands of FeCO and $\text{Fe}(\text{CO})_2$ complexes on $\text{Ag}(110)$ were found, and interpreted to be caused by the local electronic structure of the Fe atom. Our results indicate that not only the C–O bond length but also the adsorption angle can be an indicator of the charge state of the host, in our case the gold dimer.

The optimized structures of several Au_2O_2^- complexes are shown in Figure 2(a–d). As evident from Figure 2, bonding of di-oxygen to Au_2^- can take place in various ways, which may involve both Au–Au and O–O bond breaking. However, in the GS configuration (Figure 2a) oxygen is clearly molecularly and rather strongly (BE = 1.39 eV) bound to gold.²² In this “end-bonded” configuration, which is energetically 0.6 eV more stable than the first isomer (Au–O–Au–O linear chain) the O–O bond is stretched by 8%, whence the Au–Au bond length is intermediate between that of the neutral and anionic Au_2 . Spatial analysis of the electronic charge indicates a net transfer of 0.26e to oxygen,

(16) Gantefor, G. F.; Cox, D. M.; Kaldor, A. J. *Chem. Phys.* **1990**, *93*, 8395.

(17) (a) *AIP Handbook*, 3rd ed.; McGraw-Hill: New York, 1972. (b) Zhang, Y.; Yang, W. *Phys. Rev. Lett.* **1998**, *80*, 890.

(18) *CRC Handbook of Chemistry and Physics*, 55th ed.; CRC Press: Cleveland, OH, 1974.

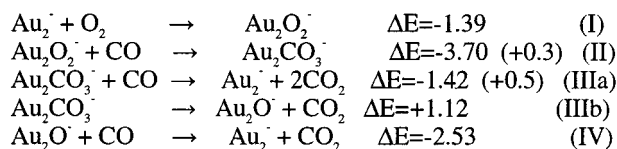
(19) Somorjai, G. A. *Introduction to Surface Chemistry and Catalysis*; Wiley-VCH: New York 1994.

(20) The calculated harmonic gas-phase CO frequency is 2140 cm^{-1} , compared to the experimental harmonic frequency of 2170 cm^{-1} . All of the reported frequencies include the correction factor of 2170/2140.

(21) Lee, H. J.; Ho, W. *Science* **1999**, *286*, 1719.

(22) O_2 binds weakly (BE = 0.45 eV) to neutral Au_2 in a structure similar to Figure 2(a) with $d(\text{O}–\text{O}) = 1.29$ Å. The molecule is not activated.

Scheme 1. A Catalytic Cycle Yielding 2 CO_2 Molecules^a



^a Each step shows the calculated energy change, ΔE , with respect to the previous step. The initial reference energy is the sum of the gas-phase energies $E(\text{Au}_2^-) + E(\text{O}_2) + 2E(\text{CO})$. Activation barriers are given in parenthesis. All the energies are in eV. A negative energy value corresponds to an exothermic step.

and the extra electron of the anionic complex promotes occupation of one of the initially half-filled $\text{O}_2(\pi^*)$ antibonding orbitals (by 0.4e), making oxygen a superoxo-like species. The stability of the GS molecular complex suggests that molecular oxygen adsorption to gold should be realizable under common experimental conditions.

We turn now to study the full catalytic cycle of oxidation of CO in the presence of Au_2^- : $\text{Au}_2^- + \text{O}_2 + 2\text{CO} \rightarrow \text{Au}_2^- + 2\text{CO}_2$ (Scheme 1). (I) is the elementary step of O_2 adsorption, which we predict to occur molecularly as shown in Figure 2a and discussed above. Adding CO from the gas phase may lead to several intermediate complexes, out of which a carbonate complex²³ Au_2CO_3^- (step II) is thermodynamically the most stable.²⁴ The formation of the carbonate involves an activation barrier of 0.3 eV.²⁵ This di-gold–carbonate is the key intermediate compound in the reaction cycle, and its experimental verification would be most interesting. Since it has a distinctively high electron detachment energy, 4.67 eV, reflecting its stability, and setting it apart from the other possible compounds of the same mass,²⁴ it should be detectable experimentally by photodepletion studies.

From the carbonate, the reaction cycle can proceed along two branches, corresponding to steps (IIIa) or (IIIb). Step (IIIa) includes reaction of a gas-phase CO with Au_2CO_3^- , which requires an activation barrier of 0.5 eV but produces simultaneously two CO_2 molecules detaching readily from gold and completing the cycle. Step (IIIb) is endothermic, requiring 1.12 eV to detach the CO_2 molecule from the carbonate; however, the remaining linear Au_2O^- is highly reactive with another gas-phase CO, producing CO_2 without an activation barrier (step IV). In both cases, the total exothermicity of the oxidation reaction is 3.25 eV per CO.

Acknowledgment. This research is supported by the U.S. AFOSR and the Academy of Finland. We thank U. Heiz and Th. Bernhardt for discussions.

JA0165180

(23) Written formally as $\text{Au}–\text{Au}–\text{O}^{(1)}–\text{CO}^{(2)}–\text{O}^{(3)}$. The bond lengths are: $d(\text{Au}–\text{Au}) = 2.56$ Å; $d(\text{Au}–\text{O}^{(1)}) = 2.09$ Å; $d(\text{O}^{(1)}–\text{C}) = 1.29$ Å; and for the two $\text{C}–\text{O}^{(2),(3)}$ bonds $d(\text{C}–\text{O}) = 1.27$ Å. The O–CO₂ plane has an angle of 127.4° with the Au–Au–O⁽¹⁾ axis, $\angle(\text{O}^{(1)}\text{CO}^{(2),(3)}) = 118.1^\circ$, and $\angle(\text{O}^{(2)}\text{CO}^{(3)}) = 123.8^\circ$.

(24) Three other structures are also energetically feasible: (i) Another carbonate, which could be formed by inserting CO in the middle of the O–O bond of Au_2O_2^- in Figure 2d, (ii) a coadsorbed $\text{OC}–\text{Au}–\text{Au}–\text{O}_2^-$, and (iii) a coadsorbed $\text{Au}–(\text{CO})–\text{Au}–\text{O}_2^-$ structure. The energy difference ΔE to the GS and vDE for these structures are: (i) $\Delta E = 1.04$ eV; vDE = 3.38 eV; (ii) $\Delta E = 2.80$ eV; vDE = 2.82 eV; (iii) $\Delta E = 2.94$ eV; vDE = 3.32 eV.

(25) Reaction barriers were determined by constrained optimizations, where the reaction coordinate x_r (distance between chosen atoms, e.g., the C atom of the approaching CO molecule and one of the O atoms of the Au_2O_2^- in step II), was changed by increments of 0.1–0.2 Å, with all other degrees of freedom fully relaxed for each value of x_r . This procedure yields the shape of the reaction barrier along the reaction path, and with the discretization of x_r used here the barrier height (and the transition state) is estimated within 0.1 eV. The connectivity between the transition state and the products in steps (II), (IIIa) was verified using first-principles dynamical simulations, releasing the system from the transition state.